

Published in final edited form as:

*Angew Chem Int Ed Engl.* 2009 ; 48(46): 8712–8715. doi:10.1002/anie.200904550.

## Apamin as a novel template for structure-based rational design of potent peptide activators of p53\*\*

**Chong Li**<sup>†</sup>,

Institute of Human Virology, University of Maryland School of Medicine, 725 W. Lombard St., Baltimore, MD 21201 (USA)

Fudan University School of Pharmacy, Shanghai (China)

**Marzena Pazgier**<sup>†</sup>[Dr.],

Institute of Human Virology, University of Maryland School of Medicine, 725 W. Lombard St., Baltimore, MD 21201 (USA)

**Min Liu**[Dr.],

Institute of Human Virology, University of Maryland School of Medicine, 725 W. Lombard St., Baltimore, MD 21201 (USA)

**Wei-Yue Lu**[Prof.], and

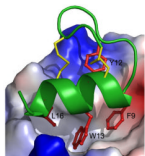
Fudan University School of Pharmacy, Shanghai (China)

**Wuyuan Lu**

Institute of Human Virology, University of Maryland School of Medicine, 725 W. Lombard St., Baltimore, MD 21201 (USA)

Wuyuan Lu: wlu@ihv.umaryland.edu

### Abstract



The oncoproteins MDM2 and MDMX negatively regulate the activity and stability of the tumor suppressor protein p53, and are important molecular targets for anticancer therapy. Grafting four residues critical for MDM2/MDMX binding to the C-terminal  $\alpha$ -helix of apamin converts the bee-venom neurotoxin into a novel class of potent p53 activators with potential antitumor activity.

### Keywords

p53; MDM2; MDMX; apamin; stingin

---

\*\*We thank Prof. Aumelas of University of Montpellier for kindly providing the coordinates for the crystal structure of apamin, and Prof. Vogelstein of Johns Hopkins University for generously providing HCT116 cells. This work was supported in part by a Research Scholar Grant CDD112858 from the American Cancer Society and the National Institutes of Health Grants AI056264 and AI061482 (to W.L.), and by China Scholarship Council (to C.L.).

Correspondence to: Wuyuan Lu, wlu@ihv.umaryland.edu.

<sup>†</sup>These authors contributed equally to this work.

Supporting information for this article is available on the WWW under <http://www.angewandte.org> or from the author.

The activity and stability of the tumor suppressor protein p53 is negatively regulated by the two oncogenic proteins MDM2 and MDMX – a cellular process initiated by MDM2/MDMX binding to the N-terminal transactivation domain of p53 [1]. MDM2 – an E3 ubiquitin ligase primarily controls p53 stability by targeting the tumor suppressor protein for ubiquitin-mediated constitutive degradation, whereas MDMX mainly functions as an effective transcriptional antagonist of p53 that blocks its ability to regulate responsive genes expression. Antagonists that block the p53-binding pocket of MDM2/MDMX kill tumor cells both *in vitro* and *in vivo* by re-activating the p53 pathway, resulting in cell cycle arrest, senescence or apoptosis [2]. Acting synergistically in tumor cells, MDM2 and MDMX have become two highly attractive molecular targets for anticancer drug development. Using phage display, we previously identified a 12-mer peptide, termed PMI (p53-MDM2/MDMX inhibitor), with low nM affinity for both MDM2 and MDMX [3]. Here we report that grafting four residues of PMI critical for MDM2/MDMX binding to apamin – a highly specific blocker of Ca<sup>2+</sup>-activated K<sup>+</sup> channels of small conductance [4], converted the 18-amino acid residue bee-venom neurotoxin to several potent peptide inhibitors of the p53-MDM2/MDMX interactions with different specificities. The rational design of these apamin-derived p53 activators, termed stingins, was structurally validated by X-ray crystallography.

The N-terminal transactivation domain of p53 encompasses the sequence T<sup>18</sup>F<sup>19</sup>S<sup>20</sup>D<sup>21</sup>L<sup>22</sup>W<sup>23</sup>K<sup>24</sup>L<sup>25</sup>L<sup>26</sup> minimally required for effective MDM2/MDMX binding [5]. Residues Phe19, Trp23 and Leu26 of p53, constituting an amphipathic  $\alpha$ -helix, dock their side chains inside a hydrophobic cavity of MDM2/MDMX, and are energetically the most critical residues for MDM2/MDMX recognition [6]. We and others have also found that Tyr22 is superior to Leu22 in contributing to MDM2/MDMX binding [3,7]. Apamin consists of an N-terminal loop and a C-terminal  $\alpha$ -helix globally stabilized by two disulfide bridges (Cys1–Cys11 and Cys3–Cys15) [8], providing an attractive structural template for *de novo* design of new functionalities [9]. To convert apamin to an inhibitor that emulates the activity of <sup>18–26</sup>p53, we grafted Phe19, Tyr22, Trp23, and Leu26 to the topologically equivalent positions of apamin in its  $\alpha$ -helical region, generating, via additional C-terminal truncation, stingins 1–5, ranging from 16 to 18 amino acid residues (Table 1). Two sets of residues in apamin were structurally permissible to the grafting: Ala9-Ala12-Arg13-Gln16 and Leu10-Arg13-Arg14-Gln17. Replacement of the former resulted in stingins 1–3, while substitutions of the latter yielded stingins 4–5. Notably, as residues Arg13, Arg14, and Gln17 are functional determinants of apamin [8], conversion to stingins is expected to conveniently decimate its neurotoxin activity. All five stingin peptides along with apamin were chemically synthesized, spontaneously and quantitatively folded within 2 hours under thiol-disulfide shuffling conditions, and purified to homogeneity by reversed-phase HPLC. All stingin peptides are highly soluble in aqueous solution. As is the case with native apamin, the C-termini of synthetic apamin and stingins are all amidated.

A previously detailed, surface plasmon resonance (SPR) based competition assay was performed to quantify the interactions between stingins and synthetic <sup>25–109</sup>MDM2 and <sup>24–108</sup>MDMX (or <sup>syn</sup>MDM2 and <sup>syn</sup>MDMX) [3,10]. The quantification technique is based on the principle that a surface immobilized <sup>15–29</sup>p53 peptide accurately measures the concentration of free (unbound) <sup>syn</sup>MDM2 or <sup>syn</sup>MDMX in an incubation solution that contains a fixed concentration of the protein with varying concentrations of test peptide. PMI and all five stingin peptides competed, in a dose-dependent manner, with immobilized <sup>15–29</sup>p53 for <sup>syn</sup>MDM2 or <sup>syn</sup>MDMX binding (Supporting Information). Nonlinear regression analyses yielded for PMI a K<sub>d</sub> value of 3.2 ± 1.1 nM for <sup>syn</sup>MDM2 and of 8.5 ± 1.7 nM for <sup>syn</sup>MDMX, in full agreement with the previously published K<sub>d</sub> values of 3.3 and 8.9 nM, respectively, determined by isothermal titration calorimetry [3]. While apamin, as expected, showed no binding to either <sup>syn</sup>MDM2 or <sup>syn</sup>MDMX, stingin peptides

bound <sup>syn</sup>MDM2 and <sup>syn</sup>MDMX effectively with  $K_d$  values ranging from 11.4 to 252 nM (Table 1). Interestingly, stingins 1–3 are MDMX-specific, giving rise to  $K_d$  values for <sup>syn</sup>MDMX 2-to-4 fold lower than those for <sup>syn</sup>MDM2. By contrast, stingins 4–5 are MDM2-specific, as evidenced by a 3-to-5 fold difference in  $K_d$  values between <sup>syn</sup>MDM2 and <sup>syn</sup>MDMX, in favour of MDM2. Deletion of the C-terminal residue(s) flanking Leu16 in stingins 1–2 (Gln17 and His18) slightly weakened MDM2/MDMX binding. Removal of His18 in stingin-4, however, significantly improved binding to both MDM2 and MDMX. Taken together, these results suggest that while the four grafted residues (Phe/Tyr/Trp/Leu) are critical for stingin-MDM2/MDMX interactions, frame shift (from stingins 1–3 to stingins 4–5) and modulation of the C-terminal residues flanking Leu16 or Leu17 fine-tune stingin activity and specificity.

The crystal structure of stingin-5 was determined at 1.48 Å resolution. As shown in Figures 1A and 1B, stingin-5 preserves a parental fold of apamin and presents an amphipathic  $\alpha$ -helix required for effective MDM2/MDMX binding. Among the four residues (Phe10, Tyr13, Trp14, and Leu17) introduced into the helical region of apamin, only Leu17 – the C-terminal residue is located outside of the regular  $\alpha$ -helix. The topology of the side chains of the four hydrophobic residues in stingin-5 is such that only minor conformational adjustments are required for its productive binding to the p53-binding cavity of MDM2/MDMX. A superposition of stingin-5 and apamin shows overlapping secondary structural elements and native disulfide bonds, with a root-mean-square deviation (rmsd) between equivalent  $C^\alpha$  atoms of 0.6–0.7 Å, structurally validating apamin as an ideal template for rational design of miniature protein inhibitors of p53-MDM2/MDMX interactions.

To better understand the molecular recognition between MDM2/MDMX and stingins, we determined the crystal structure at 1.65 Å resolution of <sup>syn</sup>MDM2 complexed with stingin-1 – a potent antagonist of both MDM2 and MDMX (Figures 1C and 1D). As expected, residues 9–17 of stingin-1 adopt an amphipathic  $\alpha$ -helical conformation, allowing the side chains of Phe9, Trp13 and Leu16 to bury deep inside the p53-binding pocket of MDM2. These three residues collectively contribute 63% of the total buried surface area (BSA) of stingin-1. Tyr12 stacks against Val93 and forms  $\pi$ -cation interactions with Lys94 and His73 of MDM2, contributing additional 17% of the total BSA.

Stingin-1 closely resembles PMI and other p53-like peptide ligands with respect to MDM2 binding [3,5a,11]. Shown in Figure 1E are overlapping stingin-1 and PMI seen in their respective complexes with (superimposed) <sup>syn</sup>MDM2. The side chains of Phe9, Tyr12, and Trp13 of stingin-1 and of Phe3, Tyr6, and Trp7 of PMI occupy identical positions in the complexes and make identical contacts with the residues of MDM2. A notable structural difference between stingin-1 and PMI centers on the  $C^\alpha$  and  $C^\beta$  atoms of Leu16 of stingin-1 and of Leu10 of PMI ( $C^\alpha$ : 2.1 Å apart;  $C^\beta$ : 2.25 Å apart), attributable to an extension, in comparison with PMI, of the  $\alpha$ -helix of stingin-1 at the C-terminus. The extension of the C-terminal  $\alpha$ -helix of stingin-1, supported by the Cys3–Cys15 disulfide bond, allows Leu16 to protrude into the p53-binding pocket earlier than Leu10 of PMI. Concomitantly, an equivalent H-bond seen in the PMI-MDM2 complex (Tyr100 O<sup>n</sup> to Leu10 O) is lost between the side chain of Tyr100 of MDM2 and Leu16 O of stingin-1 [3]. Tyr100 O<sup>n</sup> in the stingin-1-MDM2 complex forms instead a water-mediated H-bond to the side chain of Gln17 of stingin-1 (Supporting Information). Despite these differences, the geometry of the  $C^\gamma$ ,  $C^{\delta 1}$  and  $C^{\delta 2}$  atoms of Leu16 of stingin-1 is nearly identical to that of Leu10 of PMI. Superposition of FLCYWRCL of stingin-1 and FAEYWNLL of PMI – the minimally required MDM2/MDMX-binding motif yields an RMSD value of 0.6 Å between their equivalent  $C^\alpha$  atoms.

The binding affinity of stingin-5 for MDM2 is 15-fold higher than that of nutlin-3 [3] – a cis-imidazoline-derived small molecule antagonist of MDM2 that kills tumor cells at low  $\mu\text{M}$  in a p53-dependent manner [2a,2b]. However, stingin-5 showed no cytotoxicity at up to 400  $\mu\text{M}$ , presumably due to its inability to permeabilize the cell membrane. To facilitate cellular uptake of stingin-5, we covalently attached to its N-terminus a cluster of nine Arg residues all in D-enantiomeric form ( $^{\text{D}}\text{R9}$ -stingin-5). Unexpectedly,  $^{\text{D}}\text{R9}$ -stingin-5 quantitatively killed both HCT116  $p53^{+/+}$  and HCT116  $p53^{-/-}$  at 12.5  $\mu\text{M}$  ( $\text{IC}_{50} \sim 6 \mu\text{M}$ ) in a p53- and time-independent fashion, strongly suggesting a necrotic cell death mechanism (Supporting Information). p53 peptides conjugated to positively charged cell penetrating peptides (CPPs) have previously been shown to induce necrosis of tumor cells independently of p53 status [12]. The failure of stingin-5 and  $^{\text{D}}\text{R9}$ -stingin-5 to activate the p53 pathway in HCT116  $p53^{+/+}$  cells underscores the importance of the development of viable cellular delivery vehicles for peptide/protein therapeutics in general. For cargo such as p53-like peptides and stingins that contain clustered hydrophobic residues, conjugation of cationic CPPs may lead to a detergent-like molecule indiscriminately toxic against all cell types.

Three major classes of MDM2/MDMX antagonists emulating the activity of the  $^{18-26}\text{p53}$  peptide are being developed for potential therapeutic applications: low molecular weight compounds such as nutlins and MI-209 – an extensively modified spiro-oxindole compound [2a,2b], various peptidomimetics [2c], and miniature proteins such as avian pancreatic polypeptide [13], thioredoxin [14], and scorpion toxin [10]. Miniproteins are genetically deliverable and generally more resistant to proteolysis *in vivo* than linear peptides. Chen and colleagues recently demonstrated that expression via adenovirus of thioredoxin displaying the sequence of a phage-optimized peptide inhibitor of MDM2 and MDMX resulted in efficient p53 activation, cell cycle arrest, and apoptosis of tumor cells overexpressing MDM2 and MDMX [14b]. Intratumoral injection of the adenovirus also induced growth suppression of tumor xenografts in mice in a p53-dependent fashion. Compared with other miniprotein activators of p53, stingins prevail in small size, high potency, and extreme ease of chemical or recombinant production [15]. Stingins are admittedly still less potent than PMI – one of the strongest peptide antagonists ever designed for MDM2/MDMX. As disulfide bonding in stingins stabilizes a preformed amphipathic  $\alpha$ -helix, thus minimizing an entropic penalty associated with complex formation, further enhancement in binding affinity should be possible through additional sequence optimization at secondary interaction sites.

In conclusion, by grafting four hydrophobic residues, critical for MDM2/MDMX binding, to the C-terminal  $\alpha$ -helix of apamin, we successfully converted the bee-venom neurotoxin into a series of potent inhibitors of p53 interactions with MDM2 and MDMX. Structural studies by X-ray crystallography validated the mode of inhibition, that is, apamin-derived stingins directly compete with p53 for MDM2/MDMX binding. Stingins represent a novel class of p53 activators and are superior in many aspects to the existing miniprotein antagonists of MDM2/MDMX. Coupled with a therapeutically viable delivery modality, stingins may have the potential to be used as antitumor agents for clinical use.

## Experimental Section

### Synthesis of apamin and stingins

All peptides were chemically synthesized on MBHA resin using the HBTU activation and DIEA *in situ* neutralization protocol developed by Kent and colleagues for Boc chemistry [16]. Oxidative folding is described as supporting information. Peptide quantification was performed by UV measurements at 280 nm using molar extinction coefficients calculated according to the published algorithm [17].

## Surface plasmon resonance (SPR) based competition binding assay

The  $K_d$  values of PMI and stingins for  $^{syn}MDM2$  and  $^{syn}MDMX$  were determined essentially as described previously [3,10] (supporting Information).

## Crystallization, data collection, structure solution, and refinement

Buffer conditions for crystallization are provided as supporting information. Data integration and scaling, and structure solution and refinement were performed as described [3]. For stingin-5, the crystal structure of wild type apamin [8] was used as a starting model to determine initial phase information. For  $^{syn}MDM2$ -stingin-1,  $^{syn}MDM2$  coordinates extracted from the  $^{syn}MDM2$ -PMI complex structure [3] were used as a search model for molecular replacement. Data collection and refinement statistics are summarized in Table S1 (Supporting Information). The coordinates and structure factors have been deposited in the PDB with accession code 3IUX. Molecular graphics were generated using Pymol (<http://pymol.org>).

## References

1. a) Vousden KH, Lane DP. *Nat Rev Mol Cell Biol.* 2007; 8:275. [PubMed: 17380161] b) Marine JC, Dyer MA, Jochemsen AG. *J Cell Sci.* 2007; 120:371. [PubMed: 17251377] c) Toledo F, Wahl GM. *Nat Rev Cancer.* 2006; 6:909. [PubMed: 17128209]
2. a) Vassilev LT, Vu BT, Graves B, Carvajal D, Podlaski F, Filipovic Z, Kong N, Kammlott U, Lukacs C, Klein C, Fotouhi N, Liu EA. *Science.* 2004; 303:844. [PubMed: 14704432] b) Shangary S, Qin D, McEachern D, Liu M, Miller RS, Qiu S, Nikolovska-Coleska Z, Ding K, Wang G, Chen J, Bernard D, Zhang J, Lu Y, Gu Q, Shah RB, Pienta KJ, Ling X, Kang S, Guo M, Sun Y, Yang D, Wang S. *Proc Natl Acad Sci U S A.* 2008; 105:3933. [PubMed: 18316739] c) Murray JK, Gellman SH. *Biopolymers.* 2007; 88:657. [PubMed: 17427181]
3. Pazgier M, Liu M, Zou G, Yuan W, Li C, Li J, Monbo J, Zella D, Tarasov SG, Lu W. *Proc Natl Acad Sci U S A.* 2009; 106:4665. [PubMed: 19255450]
4. a) Habermann E. *Science.* 1972; 177:314. [PubMed: 4113805] b) Stocker M. *Nat Rev Neurosci.* 2004; 5:758. [PubMed: 15378036]
5. a) Kussie PH, Gorina S, Marechal V, Elenbaas B, Moreau J, Levine AJ, Pavletich NP. *Science.* 1996; 274:948. [PubMed: 8875929] b) Schon O, Friedler A, Bycroft M, Freund SM, Fersht AR. *J Mol Biol.* 2002; 323:491. [PubMed: 12381304]
6. a) Bottger A, Bottger V, Garcia-Echeverria C, Chene P, Hochkeppel HK, Sampson W, Ang K, Howard SF, Picksley SM, Lane DP. *J Mol Biol.* 1997; 269:744. [PubMed: 9223638] b) Lin J, Chen J, Elenbaas B, Levine AJ. *Genes Dev.* 1994; 8:1235. [PubMed: 7926727] c) Picksley SM, Vojtesek B, Sparks A, Lane DP. *Oncogene.* 1994; 9:2523. [PubMed: 8058315] d) Massova I, Kollman PA. *J Am Chem Soc.* 1999; 121:8133.
7. Bottger V, Bottger A, Howard SF, Picksley SM, Chene P, Garcia-Echeverria C, Hochkeppel HK, Lane DP. *Oncogene.* 1996; 13:2141. [PubMed: 8950981]
8. Le-Nguyen D, Chiche L, Hoh F, Martin-Eauclaire MF, Dumas C, Nishi Y, Kobayashi Y, Aumelas A. *Biopolymers.* 2007; 86:447. [PubMed: 17486576]
9. a) Nicoll AJ, Miller DJ, Futterer K, Ravelli R, Allemann RK. *J Am Chem Soc.* 2006; 128:9187. [PubMed: 16834392] b) Pease JH, Storrs RW, Wemmer DE. *Proc Natl Acad Sci U S A.* 1990; 87:5643. [PubMed: 2377603]
10. Li C, Liu M, Monbo J, Zou G, Yuan W, Zella D, Lu WY, Lu W. *J Am Chem Soc.* 2008; 130:13546. [PubMed: 18798622]
11. Czarna A, Popowicz GM, Pecak A, Wolf S, Dubin G, Holak TA. *Cell Cycle.* 2009; 8:1176. [PubMed: 19305137]
12. a) Kanovsky M, Raffo A, Drew L, Rosal R, Do T, Friedman FK, Rubinstein P, Visser J, Robinson R, Brandt-Rauf PW, Michl J, Fine RL, Pincus MR. *Proc Natl Acad Sci U S A.* 2001; 98:12438. [PubMed: 11606716] b) Do TN, Rosal RV, Drew L, Raffo AJ, Michl J, Pincus MR, Friedman FK,

- Petrylak DP, Cassai N, Szmulewicz J, Sidhu G, Fine RL, Brandt-Rauf PW. *Oncogene*. 2003; 22:1431. [PubMed: 12629507]
13. Kritzer JA, Zutshi R, Cheah M, Ran FA, Webman R, Wongjirad TM, Schepartz A. *Chembiochem*. 2006; 7:29. [PubMed: 16397877]
14. a) Bottger A, Bottger V, Sparks A, Liu WL, Howard SF, Lane DP. *Curr Biol*. 1997; 7:860. [PubMed: 9382809] b) Hu B, Gilkes DM, J. Chen, *Cancer Res*. 2007; 67:8810.
15. Devaux C, Knibiehler M, Defendini ML, Mabrouk K, Rochat H, Van Rietschoten J, Baty D, Granier C. *Eur J Biochem*. 1995; 231:544. [PubMed: 7649153]
16. Schnolzer M, Alewood P, Jones A, Alewood D, Kent SB. *Int J Pept Protein Res*. 1992; 40:180. [PubMed: 1478777]
17. Pace CN, Vajdos F, Fee L, Grimsley G, Gray T. *Protein Sci*. 1995; 4:2411. [PubMed: 8563639]

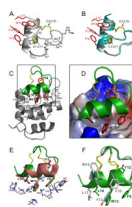



**Figure 1.**

Crystal structures of stingin-5 and of stingin-1 in complex with MDM2. **(A)** Ribbon representation of the overall structure of stingin-5. All side chains are shown as ball-sticks. Residues grafted to the apamin sequence are shown in red and disulfide bonds in yellow. **(B)** Superposition of the backbones of stingin-5 (grey) and apamin (cyan). **(C)** The co-crystal structure of synthetic <sup>25-109</sup>MDM2 (grey) and stingin-1 (green). Side chains of Phe9, Tyr12, Trp13, and Leu16 of stingin-1 are colored in red, and residues of MDM2 shaping the stingin-binding pocket shown as grey sticks. **(D)** Close-up view of the interface of the protein-peptide complex. The electrostatic potential at the molecular surface of MDM2 is displayed as negative in red, positive in blue, and apolar in white. **(E)** Stingin-1 (green) and PMI (pink), shown in a ribbon and stick representation, from their respective complexes with (superimposed) <sup>syn</sup>MDM2. Residues shown as thin sticks line the hydrophobic cavity of MDM2 - blue residues from MDM2 complexed with PMI, and grey residues from MDM2 complexed with stingin-1. **(F)** Superimposed stingin-1 (green) and stingin-5 (grey).

**Table 1**

Amino acid sequences of apamin, PMI, and stingins and their dissociation equilibrium constants for p53-binding domains of MDM2 and MDMX. Each  $K_d$  value is the mean of three independent measurements (N.B. = no binding).

Name	Sequence	$K_d$ (nM)	
		MDM2	MDMX
Apamin	CNCKAPETALCARRCQQH	N.B.	N.B.
PMI	 T <b>SFAEYW</b> NLLSP	$3.2 \pm 1.1$	$8.5 \pm 1.7$
Stingin-1	CNCKAPETFLCYWRCLQH	$25.1 \pm 5.1$	$11.4 \pm 2.3$
Stingin-2	CNCKAPETFLCYWRCLQ	$35.2 \pm 3.7$	$18.0 \pm 2.3$
Stingin-3	CNCKAPETFLCYWRCL	$57.5 \pm 7.2$	$16.0 \pm 4.5$
Stingin-4	CNCKAPETAFCAYWCQLH	$83.2 \pm 8.4$	$252 \pm 23$
Stingin-5	CNCKAPETAFCAYWCQL	$17.7 \pm 4.0$	$93.4 \pm 9.2$